Therapeutic Advances in Neurological Disorders Original Research

Distinct cerebral ^{18}F-FDG PET metabolic patterns in anti-N-methyl-D-aspartate receptor encephalitis patients with different trigger factors

Ther Adv Neurol Disord

2021, Vol. 14: 1–12

DOI: 10.1177/1756286421995635

© The Author(s), 2021.
Article reuse guidelines: sagepub.com/journals-permissions

Jingjie Ge*, Bo Deng*, Yihui Guan, Weiqi Bao, Ping Wu, Xiangjun Chen and Chuantao Zuo

Abstract

Aim: Anti-N-methyl-D-aspartate receptor (anti-NMDAR) encephalitis is a subgroup of treatable autoimmune encephalitis, characterized by rapid development of psychosis, cognitive impairments and seizures. Etiologically, anti-NMDAR encephalitis could be divided into three subgroups, which are paraneoplastic (especially associated with ovarian teratoma), viral encephalitis-related and cryptogenic. Each type is different in clinical course, treatment strategies and prognosis. In this study, we aim to investigate whether anti-NMDAR encephalitis patients with different trigger factors exhibit distinct cerebral metabolic patterns detected by ^{18}F-fluorodeoxyglucose positron emission tomography imaging.

Methods: 24 patients with anti-NMDAR encephalitis in acute phase from Huashan Hospital, Fudan University (Shanghai, China) were recruited in this study. Each patient was classified into one of etiological subgroups. Positron emission tomography images of individual patients were analyzed with both routine visual reading and computer-supported reading by comparison with those of the same 10 healthy controls using a voxel-wise statistical parametric mapping analysis.

Results: Patients in both the cryptogenic (13 patients) and paraneoplastic (five patients) subgroups showed hypermetabolism in the frontal-temporal lobes and basal ganglia, covarying with hypometabolism in the occipital regions. Notably, the abnormal metabolism was usually asymmetric in the cryptogenic subgroup, but relatively symmetric in the paraneoplastic subgroup. Moreover, the other six patients secondary to viral encephalitis presented with significant hypometabolism in the bilateral occipital regions, as well as in the unilateral temporal lobes and part of basal ganglia (also is virus infection side), but hypermetabolism in the contralateral temporal areas.

Conclusion: This study revealed that patients with anti-NMDAR encephalitis triggered by different factors presented distinct cerebral metabolic patterns. Awareness of these patterns may help to better understand the varying occurrence and development of anti-NMDAR encephalitis in each subgroup, and could offer valuable information to the early diagnosis, treatment and prognosis of this disorder.

Trial registration number ChiCTR2000029115 (Chinese clinical trial registry site, http://www.chictr.org)

Keywords: ^{18}F-fluorodeoxyglucose, anti-N-methyl-D-aspartate receptor encephalitis, autoimmune encephalitis, metabolic pattern, positron emission tomography

Received: 14 July 2020; revised manuscript accepted: 23 January 2021.

Correspondence to:
Chuantao Zuo
PET Center, Huashan Hospital, Fudan University, 518 East Wuzhong Road, Shanghai 200235, China
zuochuantao2000@126.com

Xiangjun Chen
Department of Neurology, Huashan Hospital and Institute of Neurology, Fudan University, 12 Middle Wulumuqi Road, Jing'an District, Shanghai 200040, China
xiangjchen@fudan.edu.cn

Jingjie Ge
Yihui Guan
Weiqi Bao
Ping Wu
PET Center, Huashan Hospital, Fudan University, Shanghai, China

Bo Deng
Department of Neurology, Huashan Hospital, Fudan University, Shanghai, China

*Jingjie Ge and Bo Deng contributed equally to this work.

Xiangjun Chen and Chuantao Zuo shared senior authorship.

Creative Commons Non Commercial CC BY-NC: This article is distributed under the terms of the Creative Commons Attribution-NonCommercial 4.0 License (https://creativecommons.org/licenses/by-nc/4.0/) which permits non-commercial use, reproduction and distribution of the work without further permission provided the original work is attributed as specified on the SAGE and Open Access pages (https://us.sagepub.com/en-us/nam/open-access-at-sage).

Introduction

Since the first case of anti-N-methyl-D-aspartate receptor (anti-NMDAR) encephalitis was discovered in 2005, autoimmune encephalitis related to neuronal membrane protein or synaptic protein antibodies has been reported in succession. Autoimmune encephalitis is not a rare disease, its incidence accounts for 15–20% of all encephalitis patients, with anti-NMDAR encephalitis being the most common entity at approximately 80% of autoimmune encephalitis.[1,2] A recent study has shown that the incidence of anti-NMDAR encephalitis is even higher than that of any common viral encephalitis in patient groups under 30 years old.[3]

Anti-NMDAR encephalitis is a severe but treatable autoimmune disease of the central nervous system. The occurrence of anti-NMDAR encephalitis is associated with the presence of specific antibodies against NMDAR in cerebrospinal fluid (CSF). So far, several trigger factors have been postulated in relation to the development of disease. Indeed, extracerebral tumors, ovarian teratoma in particular, were first recognized as a trigger leading to typical paraneoplastic anti-NMDAR encephalitis. More recently, observations that some patients with relapsing post-herpes simplex virus encephalitis produced NMDAR antibodies have also been confirmed by several cohort studies.[4] These patients usually present a biphasic illness pattern: the viral encephalitis course came first with clinical manifestations improved by antivirus treatment; "relapse" related to NMDAR antibodies appeared a few weeks later with even aggravated symptoms and this autoimmune encephalitis course could be relieved by immunotherapy. In addition to the two trigger factors mentioned above, the induction of NMDAR antibodies still remained uncertain in other affected patients. In this vein, the anti-NMDAR encephalitis is divided into three subgroups etiologically, which are: paraneoplastic group, viral encephalitis-related group and cryptogenic group. Each type is different in clinical course, treatment strategies and prognosis.

Conventional magnetic resonance imaging (MRI) imaging demonstrated limited values in the discernment of patients with anti-NMDAR encephalitis. Indeed, it has been reported that approximately 70% of affected patients showed normal cerebral MRI; in the remaining 30% patients with MRI abnormalities, non-specific features with diffuse or focal signals were observed.[5] By contrast, ^{18}F-fluorodeoxyglucose (^{18}F-FDG) positron emission tomography (PET) imaging has been recently recognized as a potentially useful biomarker in suspected autoimmune encephalitis.[6] In patients with anti-NMDAR encephalitis, metabolic abnormalities on ^{18}F-FDG PET in otherwise normal cerebral structures by MRI suggests that PET may be more sensitive than MRI.[7] Also, particular patterns of metabolism noted by ^{18}F-FDG PET have been described in case series with affected patients.[8,9] However, the majority of prior studies of ^{18}F-FDG PET in anti-NMDAR encephalitis were restricted to relatively small sample sizes and, more importantly, were unable to stratify the patients with trigger factors, thereby resulting in inconsistent findings.[6,8–14]

In order to explore distinct cerebral metabolic patterns underlying anti-NMDAR encephalitis with different causes, we investigated the ^{18}F-FDG PET brain imaging of affected patients in acute phase at our hospital. The regional uptake was matched with normal controls and were compared among subgroups.

Material and methods

Patients

A total of 123 outpatients or inpatients were diagnosed with anti-NMDAR encephalitis between 2014 and 2019 at Huashan Hospital, of whom 41 patients were performed with cerebral ^{18}F-FDG PET imaging. In these patients, we excluded (1) six patients without sufficient clinical information; (2) nine patients whose PET scans were not in acute phase; (3) two patients were combined with demyelinating anti-myelin oligodendrocyte glycoprotein antibodies. Finally, 24 patients were included in this study. The flow chart of enrollment is presented as Supplemental material Figure 1 online. All patients met current diagnostic criteria for anti-NMDAR encephalitis.[15]

It is notable that Kayser and Dalmau proposed a time course of anti-NMDAR encephalitis based on clinical symptoms, which divided phases of this disease into four stages, namely phase of prodrome, neuropsychiatric symptoms, neurologic complications and prolonged deficits.[16] In this study, we define the phases of neuropsychiatric

symptoms and neurologic complications as acute phase. To reduce the influence of different clinical course upon brain PET imaging, only the patients in acute phase, not the phase of prolonged deficits, were recruited according to a previous study.[16]

According to the underlying trigger factors, patients were classified into three subgroups: "paraneoplastic group", "viral encephalitis-related group" and "cryptogenic group". In the "paraneoplastic group", autoantibody was proposed to be triggered by antigens expressed by tumor. Ovarian teratoma was detected by computed tomography (CT), MRI or B-mode ultrasound and was confirmed by surgical resection. In the "viral encephalitis-related group", autoantibody was postulated to be triggered by antigens released by the viral destruction of neurons. Patients should present with biphasic illness pattern. In the first phase (viral encephalitis course), patients should meet the diagnostic criteria for encephalitis[17] and have at least one of the following features which supported the infection of virus: (1) intrathecal synthesis of specific antibodies against herpes simplex virus types 1 and 2, varicella zoster virus, cytomegalovirus and Epstein–Barr virus detected by enzyme-linked immunosorbent assay according to manufacturers' instructions (Euroimmun, Lubeck, Germany); (2) brain MRI or CSF analysis suggested brain parenchymal hemorrhage; (3) treatment response with antiviral therapy. In the second phase (autoimmune encephalitis course), antibodies against NMDAR should be detected in CSF. Patients in the "cryptogenic group" had no evidence of tumor or viral infection. All imaging data of each patient (including brain MRI and ^{18}F-FDG PET) together with demographic and clinical data were investigated. The disease severity of each patient was assessed using modified Rankin Scale (mRS). The study has been approved by the institutional review board and registered on Chinese clinical trial registry site (http://www.chictr.org, number ChiCTR2000029115). All patients have signed an informed consent form.

Finally, 10 healthy subjects with cerebral ^{18}F-FDG PET scans were retrospectively included in this study as the controls involved in comparison imaging analysis using voxel-wise statistical parametric mapping (SPM). All healthy subjects had no history of neurological and mental disorders.

Brain MRI scanning

Patients' brain MRI were acquired with a 3T MAGNETOM Verio scanner (Siemens, Germany) or 3T MR750 scanner (GE Healthcare, USA) in Huashan Hospital, Fudan University. The following sequences were obtained: axial T2-weighted images, axial T1-weighted images, fluid-attenuated inversion recovery images, diffusion-weighted images, and contrast-enhanced T1-weighted images.

^{18}F-FDG PET scanning

All subjects were asked to fast for at least 6 h, but had free access to water before PET imaging. PET scans were performed with a Siemens Biograph 64 PET/CT (Siemens, Germany) in three-dimensional (3D) mode. A CT transmission scan was first performed for attenuation correction. The emission scan was acquired between 45 min and 55 min after intravenous injection of 185 MBq of ^{18}F-FDG. All studies in patients and normal individuals were performed in a resting state in a quiet and dimly lit room. All patients and normal individuals were monitored *via* cameras and remained awake during the course of uptake and scanning procedure.

PET imaging analysis

PET imaging data were analyzed with both routine visual reading and computer-supported reading using SPM5 software (Wellcome Department of Imaging Neuroscience, Institute of Neurology, London, UK) implemented in Matlab 7.4.0 (MathWorks Inc., Sherborn, MA, USA).[18] For routine visual reading of the PET images, the scans were reconstructed, corrected for attenuation, and smoothed for each subject. ^{18}F-FDG PET images were displayed as a series of 148 transaxial slices scaled to a common maximum in a standard color scale. Activities in the cortical and subcortical structures are analyzed visually by two expert readers blinded to the clinical information.

In SPM analysis, scans from each subject were first spatially normalized into Montreal Neurological Institute brain space with linear and non-linear 3D transformations. The normalized PET images were then smoothed by a Gaussian filter of 10 mm FWHM over a 3D space to increase signal to noise ratio for statistical analysis. To characterize metabolic activity in individual patients with anti-NMDAR encephalitis

compared with control group, we performed a group comparison by using a two-sample *t*-test design according to the general linear model at each voxel. Mean signal differences over the whole brain were removed by AnCova in each individual subject. We set the peak threshold at $p < 0.05$ (uncorrected) over whole brain regions to ensure significant differences. Significant regions were finally localized by Talairach Daemon software (Research Imaging Center, University of Texas Health Science Center, San Antonio, TX, USA). The SPM t-maps for increased or decreased metabolism were overlaid on a standard T1-weighted MRI brain template in stereotaxic space.

Statistical analysis of patients' demographic and clinical data was performed with SPSS version 21 (IBM, Armonk, NY, USA). Data were presented as the mean ± standard deviation for normal distribution variables and median [interquartile range (IQR)] for non-normal distribution variables. Normal distribution data were compared by *t* test or two-way analysis of variance with Bonferroni test. Non-normal distribution data were compared by the Kruskal–Wallis test. Categorical variables were compared with Fisher exact test. A two-tailed $p < 0.05$ was considered as statistical significance.

Results

Clinical data

Twenty-four patients (17 male, 7 female) with anti-NMDAR encephalitis were finally included in this study. Patients' median age was 22 years (IQR: 17–32 years). Among 24 patients, 13 patients with anti-NMDAR encephalitis were determined as cryptogenic, five patients as paraneoplastic and the remaining six were considered secondary to virus infection of the central nervous system. The details of demographic and clinical information for individual patients are provided in Supplemental Table 1 and the comparison results among three subgroups are listed in Table 1. In general, we found that patients' onset age had no statistical difference among the three groups ($p > 0.05$). Patients in the paraneoplastic group presented with more severe symptoms (maximum mRS), higher rate of central hypoventilation and intensive care unit admission (all $p < 0.05$). On auxiliary examination, the proportion of abnormal electroencephalogram (EEG) and CSF showed no statistical difference among the three groups (both $p > 0.05$). No difference in the interval from disease onset to PET study and mRS at PET study were noted among the three groups (both $p > 0.05$). The proportion of steroids, sedatives or antiepileptic drugs usage before PET study in the three groups also had no statistical difference (all $p > 0.05$). All patients received immunotherapies, but patients in the viral encephalitis-related group had poorer outcome ($p = 0.001$).

The details of demographic information for 10 healthy subjects (eight male, two female) involved in SPM analysis are provided in Supplemental Table 2. The median age of healthy subjects was 57 years (IQR: 49–60 years). There were no significant differences in gender between the healthy subjects and patients with anti-NMDAR encephalitis ($p > 0.05$), while the average age of healthy subjects was higher than that of anti-NMDAR encephalitis patients ($p < 0.001$) because of less availability of ^{18}F-FDG PET imaging of juvenile healthy subjects.

Imaging analysis

The details of imaging results (both MRI and PET) for individual patients are provided in Table 2. For MRI imaging, we observed an overall 50% (12/24) of all patients presenting with normal MRI. Specifically, only three of the 13 patients in the cryptogenic group, three of the five patients in the paraneoplastic group, but all patients in viral encephalitis-related were observed with abnormal MRI signals, which had statistical difference ($p = 0.004$).

For ^{18}F-FDG PET imaging, we noted that 100% (24/24) of patients enrolled in the current study in each subgroup had abnormalities on PET scans, with frontal-temporal-occipital lobes and basal ganglia as the most frequently affected regions (Table 2). Figure 1 displays a typical case of a patient with cryptogenic anti-NMDAR encephalitis (Patient No. 1.5). This case had no obvious abnormality in cerebral MRI imaging, while ^{18}F-FDG PET showed widespread hyperactivities in the left frontal-temporal-parietal cortices and left basal ganglia, with diffuse hypoactivities in the bilateral occipital lobe. Figure 2 illustrates a typical case of a patient with paraneoplastic anti-NMDAR encephalitis (Patient No. 2.3). No abnormality was detected by MRI scan; however, ^{18}F-FDG

Table 1. Comparison of demographic and clinical information among the three subgroups.

Item	Cryptogenic group *n* = 13	Paraneoplastic group *n* = 5	Viral encephalitis-related group *n* = 6	*p* value
Age, years	21 (17–29)	23 (18–25)	31 (16–50)	0.906
Female	2/13	5/5	1/6	0.002
Psychiatric symptoms	12/13	5/5	6/6	1.000
Cognitive impairment	12/13	5/5	6/6	1.000
Seizures	11/13	4/5	3/6	0.387
Speech disorder	7/13	3/5	4/6	1.000
Movement disorder	5/13	5/5	4/6	0.059
Decreased level of consciousness	8/13	5/5	5/6	0.329
Autonomic dysfunction	3/13	0/5	3/6	0.171
Central hypoventilation	0/13	4/5	0/6	0.000
Maximum mRS	4 (3–4)	5 (5–5)	4 (3.8–4.3)	0.003
Admission to ICU	4/13	5/5	1/6	0.012
Abnormal CSF	8/13	2/5	6/6	0.113
Abnormal brain MRI	3/13	3/5	6/6	0.004
Abnormal EEG	8/11	4/5	2/5	0.475
Interval between onset and PET scan, weeks	6.8 ± 6.5	16.6 ± 14.9	8.3 ± 7.1	0.133
Treated with steroids before PET	9/13	4/5	3/6	0.618
Treated with sedative before PET	5/13	1/5	5/6	0.097
Treated with AEDs before PET	9/13	5/5	3/6	0.253
mRS at the time of PET	3 (2–3)	2 (2–3.5)	3 (3–3.2)	0.180
Interval between onset and immunotherapies, days	17.5 ± 15.8	9.4 ± 3.6	38.3 ± 35.4	0.073
First-line treatment	13/13	5/5	6/6	1.000
Second-line treatment	9/13	0/5	4/6	0.031
Follow-up time, years	2.6 ± 1.2	4.4 ± 1.5	3.0 ± 1.4	0.059
mRS at the last follow-up	0 (0–1)	0 (0–1)	2 (2–2)	0.001

AED, antiepileptic drug; CSF, cerebrospinal fluid; EEG, electroencephalogram; ICU, intensive care unit; MRI, magnetic resonance imaging; mRS, modified Rankin Scale; PET, positron emission tomography.

imaging showed symmetrical hypermetabolism in bilateral temporal lobe and basal ganglia, with diffuse hypometabolism in bilateral parieto-occipital lobe. Figure 3 demonstrated a typical case of a patient with anti-NMDAR encephalitis secondary to viral encephalitis (Patient No. 3.4). We observed atrophy in the right temporal lobe especially in the hippocampus with abnormal signals and

Table 2. The details of imaging results for individual patients.

Anti-NMDAR encephalitis	Gender	Age, years	Cerebral MRI imaging	^{18}F-FDG PET imaging									
				Left cerebral					Right cerebral				
				Frontal	Temporal	Basal ganglia	Parietal	Occipital	Frontal	Temporal	Basal ganglia	Parietal	Occipital
Cryptogenic group (13 cases)													
1.1	F	19	Enlarged left ventricular temporal angle	–	↑	–	–	↓	–	–	–	–	↓
1.2	M	33	Normal	–	–	–	–	↓	↑	↑	↑	–	↓
1.3	M	67	Bilateral frontal, parietal and paraventricular small infarcts, mild cerebral atrophy	–	–	–	↓	↓	↑	↑	↑	↓	↓
1.4	M	18	Normal	↑	↑	↑	↓	↓	–	–	–	↓	↓
1.5	M	21	Normal	↑	↑	↑	↑	↓	–	–	–	–	↓
1.6	M	24	Normal	↑	↑	–	–	↓	–	–	–	–	↓
1.7	F	21	Normal	–	–	–	–	–	↑	↑	↑	↑	–
1.8	M	25	Normal	–	↑	↑	–	↓	–	–	–	–	↓
1.9	M	24	Normal	–	–	–	–	↓	↑	↑	–	–	↓
1.10	M	15	Normal	–	↑	–	–	–	↑	↑	–	–	↓
1.11	M	58	Abnormal signals in the bilateral fronto-temporal lobe and corpus callosum	↑	–	–	↑	↓	↑	–	–	–	↓
1.12	M	16	Normal	–	↑	↑	↑	–	–	↑	–	–	↓
1.13	M	14	Normal	–	–	↑	–	↓	–	–	↑	–	↓
Paraneoplastic group (five cases)													
2.1	F	16	Multifocal abnormal signals in the bilateral parietal and lateral ventricle	–	↑	↑	↓	–	–	↑	↑	↓	–
2.2	F	23	Bilateral temporal lobe (mainly hippocampus) atrophy with abnormal signals	–	↑	↑	–	↓	–	↑	↑	–	↓
2.3	F	20	Normal	–	↑	↑	↓	↓	–	↑	↑	↓	↓

(Continued)

Table 2. (Continued)

Anti-NMDAR encephalitis	Gender	Age, years	Cerebral MRI imaging	^{18}F-FDG PET imaging									
				Left cerebral					Right cerebral				
				Frontal	Temporal	Basal ganglia	Parietal	Occipital	Frontal	Temporal	Basal ganglia	Parietal	Occipital
2.4	F	27	Abnormal signals of bilateral temporal lobe (mainly hippocampus)	–	↑	↑	–	–	–	↑	↑	–	–
2.5	F	23	Normal	–	–	↑	–	↓	–	–	↑	–	↓
Viral encephalitis-related group (six cases)													
3.1	F	16	Abnormal signals in the left temporal lobe, hippocampus and left basal ganglia	–	↓	↓	–	–	–	↑	↑	–	–
3.2	M	43	Abnormal signals in the right temporo-parietal lobe	–	↑	–	–	–	–	↓	–	↓	–
3.3	M	69	Swelling of right temporal (including insula and hippocampus) with abnormal signals	–	–	↑	–	–	–	↓	↓	–	–
3.4	M	44	Right temporal lobe/hippocampus atrophy with abnormal signals and hemorrhagic lesions	–	↑	–	–	–	–	↓	–	↓	↓
3.5	M	16	Bilateral fronto-temporal lobe, left occipital and cingulate gyrus swelling with abnormal signals	↓	↓	–	–	↓	↓	–	↑	–	–
3.6	M	18	Abnormal signals of right temporo-parietal lobe	–	↑	↑	–	–	↓	↓	–	↓	–

↑, increased metabolism; ↓, decreased metabolism; –, no changes.
^{18}F-FDG PET, ^{18}F-fluorodeoxyglucose positron emission tomography; anti-NMDAR, anti-N-methyl-D-aspartate receptor; F, female; M, male; MRI, magnetic resonance imaging.

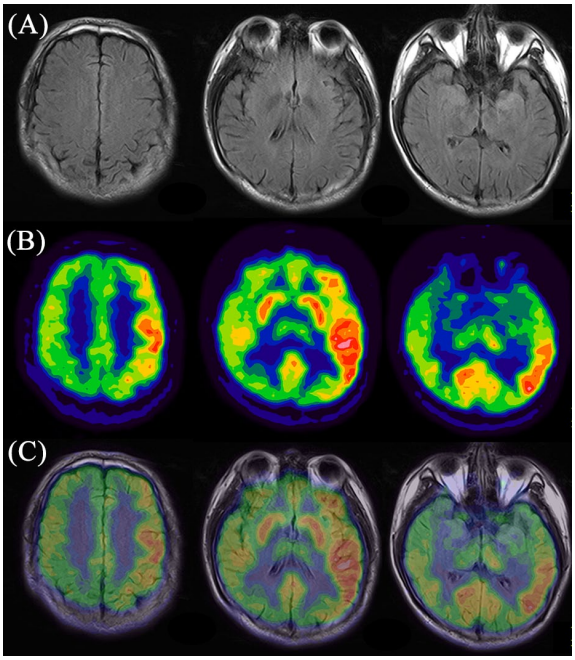

Figure 1. Representative images of abnormal cerebral glucose metabolism in patient with cryptogenic anti-NMDAR encephalitis detected by ^{18}F-FDG PET imaging and corresponding MRI imaging. (A) MRI imaging; (b) ^{18}F-FDG PET imaging; (c) PET/MRI fusion imaging.
^{18}F-FDG PET, ^{18}F-fluorodeoxyglucose positron emission tomography; anti-NMDAR, anti-N-methyl-D-aspartate receptor; MRI, magnetic resonance imaging.

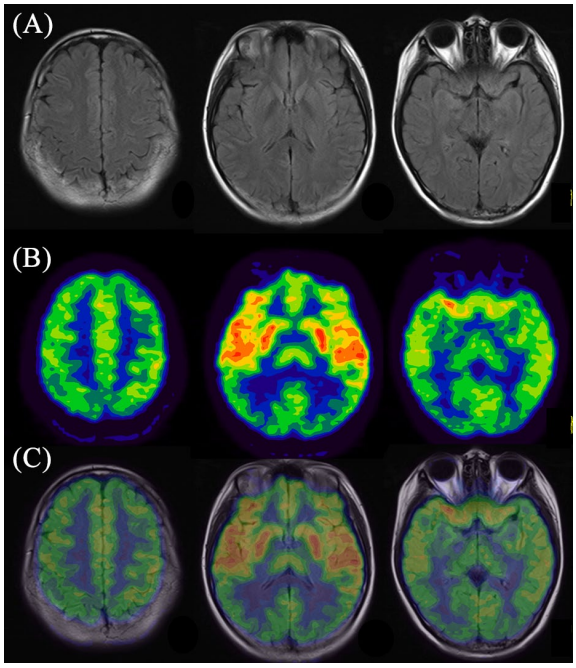

Figure 2. Representative images of abnormal cerebral glucose metabolism in patient with paraneoplastic anti-NMDAR encephalitis detected by ^{18}F-FDG PET imaging and corresponding MRI imaging. (A) MRI imaging; (B) ^{18}F-FDG PET imaging; (C) PET/MRI fusion imaging.
^{18}F-FDG PET, ^{18}F-fluorodeoxyglucose positron emission tomography; anti-NMDAR, anti-N-methyl-D-aspartate receptor; MRI, magnetic resonance imaging.

hemorrhagic lesions. Accordingly, ^{18}F-FDG PET imaging showed decreased metabolism of the right temporal lobe as well as part of the right parieto-occipital lobe, covarying with relatively increased metabolism of the contralateral temporal lobe.

The normalized PET scans of each individual patient in the three subgroups, with group comparison with 10 healthy controls using SPM analysis, further confirmed distinct characteristics of anti-NMDAR triggered by different factors. For visualization of the *t* score statistics (SPM t-map), significant voxels were projected onto a standard T1-weighted MRI brain template in stereotaxic space (Figure 4). In general, patients in the cryptogenic group showed an obvious asymmetric cerebral metabolic pattern, which commonly involved hypermetabolism in the unilateral frontal-temporal lobes and basal ganglia, covarying with diffused hypometabolism in the occipital regions. In the paraneoplastic patient group with teratoma, we observed a generally symmetric metabolic pattern featured by increased metabolism in the bilateral temporal lobes and basal ganglia, associated with decreased metabolism in the parieto-occipital regions. In the patient group secondary to viral encephalitis, focal reductions of metabolism in unilateral cerebral cortex were found, mostly affecting the unilateral temporal lobe and part of basal ganglia (the same regions with abnormal signal on MRI), accompanied by slight hypermetabolism in the contralateral temporal regions.

Discussion

This is the first study to identify distinct cerebral metabolic patterns in anti-NMDAR encephalitis patients triggered by different factors. There have been several previous reports that have described abnormal glucose metabolism in patients with autoimmune encephalitis in respect to normal control subjects. These earlier PET studies commonly demonstrated a general pattern of ^{18}F-FDG abnormalities associated with disease, or focused on pattern variations of metabolic characteristics correlating with clinical course or symptom severity

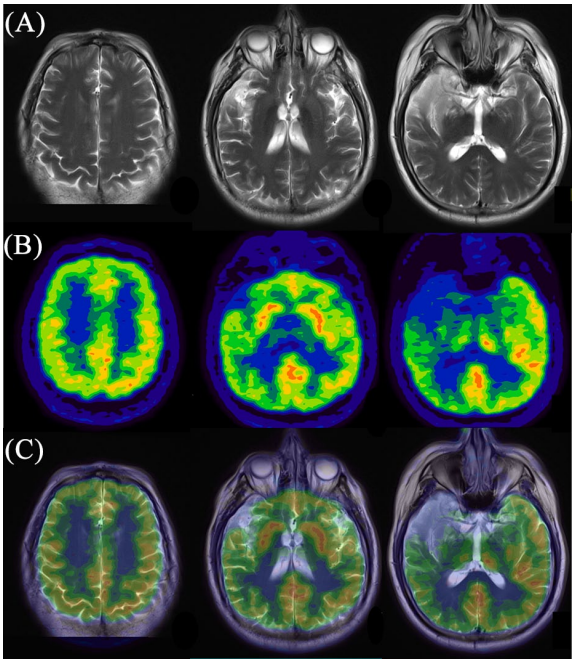

Figure 3. Representative images of abnormal cerebral glucose metabolism in patient with anti-NMDAR encephalitis secondary to viral encephalitis detected by ^{18}F-FDG PET imaging and corresponding MRI imaging. (A) MRI imaging; (B) ^{18}F-FDG PET imaging; (c) PET/MRI fusion imaging.
^{18}F-FDG PET, ^{18}F-fluorodeoxyglucose positron emission tomography; anti-NMDAR, anti-N-methyl-D-aspartate receptor; MRI, magnetic resonance imaging.

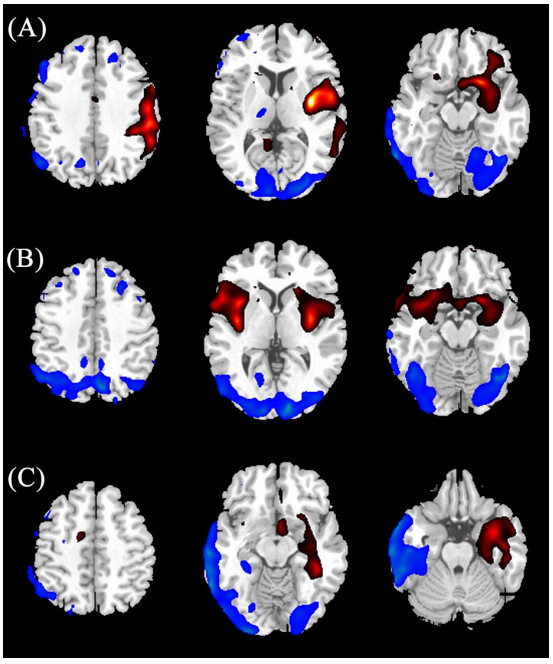

Figure 4. Results of two-sample *t* test group analysis using SPM5 for individual scans in each subgroup comparing with healthy control. The significant metabolic change regions were displayed onto a standard T1-weighted magnetic resonance imaging brain template in stereotaxic space ($p < 0.05$, uncorrected). The relatively hypermetabolic (red color) and relatively hypometabolic regions (blue color) were displayed in cryptogenic patient (A), paraneoplastic patient (B) and viral encephalitis-related patient (C), respectively.

without concerning the causes underlying anti-NMDAR encephalitis. Here, this study gave an insight to investigate anti-NMDAR encephalitis from a new etiological perspective which might be useful to facilitate early diagnosis and, more importantly, to improve treatment strategies.

The current diagnostic framework for autoimmune encephalitis has particularly distinguished anti-NMDAR encephalitis as an independent entity apart from other subtypes.[15] One main reason is that variable manifestations of anti-NMDAR encephalitis often exceeded those of classic limbic encephalitis, suggesting widespread dysfunction of neuronal activities of the whole brain. Nonetheless, many symptoms in affected patients were not correlated on MRI imaging. Indeed, it has been reported that about 70% of patients with anti-NMDAR encephalitis are normal in cerebral MRI.[5] In our study, we observed half of the patients presenting with normal MRI; however, with regard to the cryptogenic group, the proportion of MRI negative was as high as 77% and was similar to prior findings. In contrast to the poor sensitivity of MRI, we noted that all patients enrolled in the current study in each subgroup have abnormalities on ^{18}F-FDG PET scans in the acute phase with widespread involvements, indicating the neuronal dysfunction in the absence of structural disturbance. Such comparison results reminded us that when MRI negative but abnormal ^{18}F-FDG imaging presented in suspected patients with encephalitis, anti-NMDAR encephalitis should be alerted, with detection of specific antibody to be given as early as possible.

^{18}F-FDG PET results for anti-NMDAR encephalitis have been inconsistent in reported case series[6,8–14] and we considered that the discrepancies may due to different causes underlying anti-NMDAR encephalitis. The most observed abnormalities in the active phase of anti-NMDAR encephalitis consisted of increased metabolism in

anterior regions of frontal-temporal lobes relative to a decreased metabolism in posterior regions.[8,9,11] In this study, analogous ^{18}F-FDG changes in similar cortical regions were detected in patients of both cryptogenic and paraneoplastic groups. Further, our results highlighted the marked asymmetry of cortical hypermetabolism in cryptogenic patients compared with a relatively symmetric pattern which was found in the latter group. Interestingly, in line with such PET findings, we also noted that most of our cryptogenic patients presented with unilateral abnormalities in clinical symptoms or EEG, namely, focal dystonia and seizures or unilateral slow wave and epileptiform activity, supporting the patients with regional brain abnormalities. By contrast, patients in the paraneoplastic group often showed symmetry symptoms and EEG results, which further indicated highly correlation of PET characteristics with other clinical measures.

Few studies have been reported with regard to anti-NMDAR encephalitis secondary to viral encephalitis by ^{18}F-FDG imaging. Our study illustrated that patients with anti-NMDAR encephalitis triggered by virus encephalitis had a specific metabolic pattern. We noted that areas of regional hypometabolism in the unilateral temporal lobe have correlates on MRI, suggesting the possibility of impaired neuronal activities as a result of acute necrosis in neurons caused by viral encephalitis; on the other hand, the hypermetabolism in the contralateral temporal regions is more likely to be generated with attacks by autoantibodies in the second phase of the illness pattern. In addition, Novy *et al.*[12] emphasized involvements of subcortical structures in anti-NMDAR encephalitis, proposing that enhanced activities in the basal ganglia were mediated by the autoantibodies and lead to the occurrence of movement symptoms. In this context, it was plausible that the hypermetabolism of the basal ganglia in our patients of all three subgroups may reflect this aspect.

The pathophysiological basis of metabolic signatures in patients with anti-NMDAR encephalitis still remains unclear. Previous autopsy studies have confirmed that moderate brain inflammation with infiltration of plasma cells and deposits of IgG, instead of evidence of neuronal loss, occurred in patients' brain parenchyma.[19] In addition, *in vitro* and animal studies observed that antibodies against NMDAR could strongly influence the distribution and channel properties of NMDAR,[20,21] highly indicating the probability that direct pathogenic effects of autoantibodies might be the major mechanism underlying the disease.[5] Further support for this hypothesis stems from the fact that the use of ketamine, an NMDAR antagonist, could induce similar clinical symptoms in encephalitis and, moreover, facilitate an increased frontal-to-occipital gradient of glucose metabolism which mimicked the metabolic pattern observed in our affected patients.[9] However, the link between the molecular mechanism of NMDAR dysfunction and the change of whole brain metabolism still warrants further investigation.

A few limitations of this study should be noted. First, anti-NMDAR encephalitis follows a cyclical evolution process from acute stage to recovery stage, with different brain metabolic characteristics possibly occurring in each stage of disease. In the absence of follow-up observation, the current study emphasized investigation of patients only in the acute phase. This decision was a valuable strategy that helped us to eliminate potential influences on PET scans exerted by different courses of disease. However, longitudinal studies in patients with different trigger factors need to be done. Second, we conducted this study in a single institution and the sample size in the current study was relatively small due to the relatively low prevalence of disease and high costs of PET scans incurred. It will be still necessary to replicate the imaging results reported here concerning the comparisons of each subgroup with healthy subjects and to investigate group comparisons among patients with different trigger factors of anti-NMDAR encephalitis with larger sample sizes. Third, some patients recruited in this study experienced seizures several days before PET scans, and most patients had received medications such as steroids, sedatives and antiepileptic drugs before PET scans. While patients' symptom and medication may have some impact on PET imaging, it might be justifiable given that this reflected how encephalitis is diagnosed and treated in the real world. Moreover, we did not include patients after viral encephalitis as controls, which might influence the full explanation of the result of patients with anti-NMDAR encephalitis secondary to viral encephalitis. Finally, because of the lower availability of ^{18}F-FDG PET imaging of juvenile healthy subjects, the average age of healthy subjects involved in SPM analysis in the current study is higher than

that of the patients, which might have potential impact on relevant results.

At present, there are at least three reasons encouraging the extensive application of cerebral PET imaging in patients with anti-NMDAR encephalitis. First of all, whole-body ^{18}F-FDG PET imaging is frequently performed in patients with autoimmune encephalitis for screening potential malignancy. Such whole-body imaging could be easily extended to brain without adding extra radiation exposure. Second, the relapse of anti-NMDAR encephalitis has been reported as high as 20–25% and may occur repeatedly in individual patients.[22] Antibodies against NMDAR may exist in patients even after recovery, thereby having limits in predicting the relapse of disease.[23] ^{18}F-FDG scans are potential to be useful in predicting the relapse of disease in consideration of its high sensitivity. Last but not least, in the past few years, many groups have started to use PET/MRI scanners instead of single modality imaging in diagnostic algorithm for brain disorders. The application of PET/MRI imaging, especially combined with newly developed radionuclide imaging agents such as ^{18}F-GE179 targeted at NMDAR,[24] may allow us to observe specific molecular changes underlying the autoimmune encephalitis, as well as its real-time variations as disease evolves.

Conclusion

This study gave detailed descriptions of distinct brain metabolic patterns related to patients with anti-NMDAR encephalitis triggered by different causes. These metabolic patterns with ^{18}F-FDG PET scans, rather than MRI imaging, demonstrated high sensitivity associated with the disease, particularly in the cryptogenic and paraneoplastic subgroups. The awareness of such distinct patterns provided valuable information to better understand the various occurrences and development of anti-NMDAR encephalitis in each subgroup, and may help to facilitate early diagnosis, treatment strategy and prognosis prediction of this elusive, but treatable, disorder.

Author contributions

Jingjie Ge and Bo Deng, drafting and revising the manuscript, interpretation of data. Yihui Guan, revising the manuscript, acquisition and interpretation of data. Weiqi Bao, acquisition and interpretation of data. Ping Wu, acquisition and interpretation of data. Xiangjun Chen and Chuantao Zuo, conceptualization of the study, revising the manuscript, analysis and interpretation of data. All authors read and approved the final manuscript.

Availability of data and material

The datasets generated during and/or analyzed during the current study are available from the corresponding author on reasonable request.

Conflict of interest statement

The authors declare that there is no conflict of interest.

Ethics statement

All procedures performed in studies involving human participants were in accordance with the 1964 Declaration of Helsinki and its later amendments. The study has been approved by the institutional review board of Huashan Hospital and was prospectively registered on a WHO-approved Chinese clinical trial registry site (http://www.chictr.org, number ChiCTR2000029115). All subjects have signed an informed consent form.

Funding

The authors disclosed receipt of the following financial support for the research, authorship, and/or publication of this article: The study was supported by the National Natural Science Foundation of China (Nos. 81971641, 81902282), Shanghai Sailing Program funded by Shanghai Science and Technology Committee (No. 18YF1403100), Subject of Basic Research Project of "Innovation Action Plan" funded by Shanghai Science and Technology Committee (No. 201409001400) and the Shanghai Municipal Science and Technology Major Project (No. 2018SHZDZX01) and ZJLab.

Supplemental material

Supplemental material for this article is available online.

ORCID iD

Chuantao Zuo https://orcid.org/0000-0002-8856-7217

References

1. Suh-Lailam BB, Haven TR, Copple SS, *et al.* Anti-NMDA-receptor antibody encephalitis:

performance evaluation and laboratory experience with the anti-NMDA-receptor IgG assay. *Clinica Chimica Acta* 2013; 421: 1–6.

2. Davies G, Irani SR, Coltart C, *et al.* Anti-N-methyl-D-aspartate receptor antibodies: a potentially treatable cause of encephalitis in the intensive care unit. *Crit Care Med* 2010; 38: 679–682.
3. Gable MS, Sheriff H, Dalmau J, *et al.* The frequency of autoimmune N-methyl-D-aspartate receptor encephalitis surpasses that of individual viral etiologies in young individuals enrolled in the California encephalitis project. *Clin Infect Dis* 2012; 54: 899–904.
4. Armangue T, Moris G, Cantarin-Extremera V, *et al.* Autoimmune post-herpes simplex encephalitis of adults and teenagers. *Neurology* 2015; 85: 1736–1743.
5. Dalmau J and Graus F. Antibody-mediated encephalitis. *N Engl J Med* 2018; 378: 840–851.
6. Probasco JC, Solnes L, Nalluri A, *et al.* Abnormal brain metabolism on FDG-PET/CT is a common early finding in autoimmune encephalitis. *Neurol Neuroimmunol Neuroinflamm* 2017; 4: e352.
7. Morbelli S, Djekidel M, Hesse S, *et al.* Role of (18)F-FDG-PET imaging in the diagnosis of autoimmune encephalitis. *Lancet Neurol* 2016; 15: 1009–1010.
8. Yuan J, Guan H, Zhou X, *et al.* Changing brain metabolism patterns in patients with ANMDARE: serial 18F-FDG PET/CT findings. *Clin Nucl Med* 2016; 41: 366–370.
9. Leypoldt F, Buchert R, Kleiter I, *et al.* Fluorodeoxyglucose positron emission tomography in anti-N-methyl-D-aspartate receptor encephalitis: distinct pattern of disease. *J Neurol Neurosurg Psychiatry* 2012; 83: 681–686.
10. Tripathi M, Tripathi M, Roy SG, *et al.* Metabolic topography of autoimmune non-paraneoplastic encephalitis. *Neuroradiology* 2018; 60: 189–198.
11. Probasco JC, Solnes L, Nalluri A, *et al.* Decreased occipital lobe metabolism by FDG-PET/CT: an anti-NMDA receptor encephalitis biomarker. *Neurol Neuroimmunol Neuroinflamm* 2018; 5: e413.
12. Novy J, Allenbach G, Bien CG, *et al.* FDG-PET hyperactivity pattern in anti-NMDAr encephalitis. *J Neuroimmunol* 2016; 297: 156–158.
13. Baumgartner A, Rauer S, Mader I, *et al.* Cerebral FDG-PET and MRI findings in autoimmune limbic encephalitis: correlation with autoantibody types. *J Neurol* 2013; 260: 2744–2753.
14. Kerik-Rotenberg N, Diaz-Meneses I, Hernandez-Ramirez R, *et al.* A metabolic brain pattern associated with anti-N-Methyl-D-Aspartate receptor encephalitis. *Psychosomatics* 2020; 61: 39–48.
15. Graus F, Titulaer MJ, Balu R, *et al.* A clinical approach to diagnosis of autoimmune encephalitis. *Lancet Neurol* 2016; 15: 391–404.
16. Kayser MS and Dalmau J. Anti-NMDA receptor encephalitis in psychiatry. *Curr Psychiatry Rev* 2011; 7: 189–193.
17. Venkatesan A, Tunkel AR, Bloch KC, *et al.* Case definitions, diagnostic algorithms, and priorities in encephalitis: consensus statement of the international encephalitis consortium. *Clin Infect Dis* 2013; 57: 1114–1128.
18. Ge J, Wu P, Peng S, *et al.* Assessing cerebral glucose metabolism in patients with idiopathic rapid eye movement sleep behavior disorder. *J Cereb Blood Flow Metab* 2015; 35: 2062–2069.
19. Martinez-Hernandez E, Horvath J, Shiloh-Malawsky Y, *et al.* Analysis of complement and plasma cells in the brain of patients with anti-NMDAR encephalitis. *Neurology* 2011; 77: 589–593.
20. Ladepeche L, Planaguma J, Thakur S, *et al.* NMDA receptor autoantibodies in autoimmune encephalitis cause a subunit-specific nanoscale redistribution of NMDA receptors. *Cell Rep* 2018; 23: 3759–3768.
21. Kreye J, Wenke NK, Chayka M, *et al.* Human cerebrospinal fluid monoclonal N-methyl-D-aspartate receptor autoantibodies are sufficient for encephalitis pathogenesis. *Brain* 2016; 139: 2641–2652.
22. Dalmau J, Lancaster E, Martinez-Hernandez E, *et al.* Clinical experience and laboratory investigations in patients with anti-NMDAR encephalitis. *Lancet Neurol* 2011; 10: 63–74.
23. Gresa-Arribas N, Titulaer MJ, Torrents A, *et al.* Antibody titres at diagnosis and during follow-up of anti-NMDA receptor encephalitis: a retrospective study. *Lancet Neurol* 2014; 13: 167–177.
24. Yue X, Xin Y, Chugani HT, *et al.* Automated production of a N-methyl-D-aspartate receptor radioligand [^{18}F]GE179 for clinical use. *Appl Radiat Isot* 2019; 148: 246–252.

Visit SAGE journals online journals.sagepub.com/home/tan

SAGE journals